Agricultural and Forest Meteorology 306 (2021) 108451

Contents lists available at ScienceDirect

Agricultural and Forest Meteorology

journal homepage: www.elsevier.com/locate/agrformet

Watershed scale patterns and controlling factors of ecosystem respiration and methane fluxes in a Tibetan alpine grassland

Yang Li [a], Genxu Wang [a,b], Haijian Bing [b], Tao Wang [b], Kewei Huang [b], Chunlin Song [a], Xiaopeng Chen [c], Zhaoyong Hu [a], Pengfei Rui [d], Xiaoyan Song [e], Ruiying Chang [b,*]

[a] State Key Laboratory of Hydraulics and Mountain River Engineering, College of Water Resource and Hydropower, Sichuan University, Chengdu, Sichuan, China
[b] Key Laboratory of Mountain Surface Processes and Ecological Regulation, Institute of Mountain Hazards and Environment, Chinese Academy of Sciences, Chengdu, 610041, China
[c] College of Grassland Science, Shanxi Agricultural University, Taigu 030801, China
[d] Beiluhe Observation and Research Station on Frozen Soil Engineering and Environment in Qinghai-Tibet Plateau, Northwest Institute of Eco-Environment and Resources, Chinese Academy of Sciences, Lanzhou 730000, China
[e] Institute of Qinghai-Tibetan Plateau, Southwest Minzu University, Chengdu 610041, China

ARTICLE INFO

Keywords:
Methane sink
Permafrost
Terrain
Tibetan Plateau
Watershed scale

ABSTRACT

Ecosystem respiration (Re) and methane (CH_4) fluxes are two important soil-atmosphere carbon exchange processes that have been well documented at the local scale. However, the spatial patterns and controlling factors of these processes remain unclear in the Tibetan alpine permafrost region at the watershed scale. We conducted a two-year field monitoring study of Re and CH_4 fluxes at three altitudinal positions on shady and sunny slopes in a Tibetan alpine grassland to determine the spatial variability in the two processes and to identify their underlying mechanisms. The microbial factor had a controlling effect on Re spatial variability in alpine grassland watersheds. The lower soil temperature and soil organic matter content at the upper slope positions on the shady slopes inhibited Re because they reduced the soil microbial activity. We found that the alpine grassland to be a net sink of atmospheric CH_4, and the average CH_4 flux rates exhibited large spatial variance ranging from −1.60 to −10.48 μg CH_4 m^{-2} h^{-1} within the watersheds. The spatial variability in soil volumetric water content explained 76% of the variation in CH_4 fluxes within the watersheds. We suggest that the influence of permafrost on hydrologic conditions may increase the spatial variability of soil moisture (measured as soil volumetric water content and water-filled pore space) in alpine grassland watersheds, and generally form poorly drained landscape at the lower slope position where Re and CH_4 uptake are inhibited. Our results highlight the indirect effects of terrain and permafrost on Re and CH_4 fluxes through their effects on biophysiochemical factors. We recommend that the spatial variability in Re and CH_4 fluxes at the watershed scale of Tibetan alpine grassland should be given more attention in earth system models, especially the variability of CH_4 fluxes with altitudinal position.

1. Introduction

Covering approximately 24% of the global land area, mountains are complex ecological systems that have unique structures and functions (Rahbek et al., 2019). In mountains, the terrain redistributes heat and moisture, which affects soil nutrient status and plant species and forms different landscapes. For example, within watersheds, hillsides are typically eroded and dry, whereas the lowlands accumulate fertile soil and are moist (Fan et al., 2019; Philben et al., 2020). Given the high spatial variability that exists in mountainous areas, ecological experiments should consider microclimatic components by synthesising proxy variables, such as the slope aspect and altitudinal position (Carletti et al., 2009; Fan et al., 2019).

Carbon dioxide (CO_2) and methane (CH_4) are two major greenhouse gases that contribute to total radiative forcing (IPCC, 2013), and ecosystem respiration (Re) is a major pathway for CO_2 efflux from ecosystem to the atmosphere. Permafrost regions represent one of the largest soil organic carbon pools globally (Schuur et al., 2015). Recently, the dynamics, magnitudes, and controlling factors of Re and CH_4 fluxes in permafrost regions have received particular attention owing to the rapidity of climate change and large carbon stocks (Xue et al., 2016; Oh et al., 2020; Mu et al., 2020; Turetsky et al., 2020).

* Corresponding author.
E-mail address: changruiying@imde.ac.cn (R. Chang).

https://doi.org/10.1016/j.agrformet.2021.108451
Received 26 September 2020; Received in revised form 23 April 2021; Accepted 26 April 2021
Available online 13 May 2021

The Tibetan Plateau, with about 1.06 × 10^6 km^2 permafrost areas (Zou et al., 2017), accounting for more than half of the total area of alpine permafrost in the Northern Hemisphere (Yang et al., 2010; Ding et al., 2019). Due to its high altitude (> 4000 m a.s.l), this region is considered as one of the most susceptible regions to climate change (Yang et al., 2019; Mu et al., 2020). Approximately 60% of the Tibetan Plateau area are covered by mountains (Cao et al., 2011). Niu et al. (2017) reported that slope aspect and altitudinal position could alter the spatial distribution of soil temperature, soil moisture, and vegetation composition in an alpine grassland on hills, which may cause spatial variability in Re and CH_4 fluxes at the landscape scale (Treat et al., 2018; Philben et al., 2020). Although high-precision data of the slope aspect and altitudinal position can be readily obtained from digital elevation model imagery, the spatial patterns and controlling factors of Re and CH_4 fluxes on the Tibetan Plateau remain unclear at the watershed scale. This limits the accurate assessment of carbon exchange, which is problematic because watersheds are fundamental geomorphological units of the Tibetan Plateau. Consequently, studying the spatial variability and controlling factors of Re and CH_4 fluxes in Tibetan alpine grassland within watershed areas is required for accurate assessment of Tibetan Plateau permafrost carbon exchange.

We conducted a field experiment to measure the Re and CH_4 fluxes on slopes with different aspects [north-facing (shady) and south-facing (sunny) slopes], and in different altitudinal positions (lower, middle, and upper slope positions) during two consecutive growing seasons (2017 and 2018). Our study aimed to elucidate the patterns of Re and CH_4 fluxes and to quantify the relative contributions of abiotic and biotic factors in regulating Re and CH_4 fluxes at the watershed scale of a Tibetan alpine grassland.

2. Materials and methods

2.1. Study area and experimental design

The study area was located on Mt. Fenghuo (34°40′–34°46′ N and 92°50′–92°62′ E; 4580–5410 m a.s.l.; Fig. 1a), which is a continuous permafrost region in the hinterland of the Tibetan Plateau. The slopes of the study area vary between 10° and 15°. The mean annual air temperature and precipitation from 1975 to 2005 were −5.3 °C and 269.7 mm, respectively (Wang et al., 2008b). In 2017 and 2018, the mean annual air temperature was −4.6 °C and the mean annual precipitation was 383.5 mm (Fig. S1). The vegetation in the study area is predominantly alpine meadow (cold meso-perennial herbs), which covers approximately 70% of the land surface (Li et al., 2011), with the dominant alpine meadow plant species *Kobresia humilis* and *K. pygmaea* mostly distributed on the hillsides and uplands (Zhang et al., 2017). Alpine swamp meadow (hardy perennial hygrophilous herbs) that commonly occurs in river valleys, lakesides, and depressions (Wang et al., 2008b; Li et al., 2011), covers approximately 6.5% of the study area, with *K. tibetica* the dominant plant species. (Zhang et al., 2017). The study area soil type is classified as a Cryosol according to the World Reference Base for Soil Resources or a Gelisol using the United States Department of Agriculture classification system (Lessovaia et al., 2013; Bockheim and Munroe, 2014). The permafrost thickness in the study area is 60–120 m and the thickness of the active layer is 1.3–2.5 m under different terrain conditions (Fig. S2). The maximum depth of thawing is reached annually in October.

In June 2017, 18 study plots (3 × 3 m) were set up at three altitudinal positions on shady and sunny slopes in two gullies on Mt. Fenghuo (Fig. 1b; Table 1). Of the 18 study plots, twelve were located in Gully 1 and six in Gully 2. In Gully 1, two study plots, 80 m apart, were positioned at each altitude, whereas one study plot was located at per altitudinal position in Gully 2 (Fig. 1b). Three replicate polyvinyl chloride

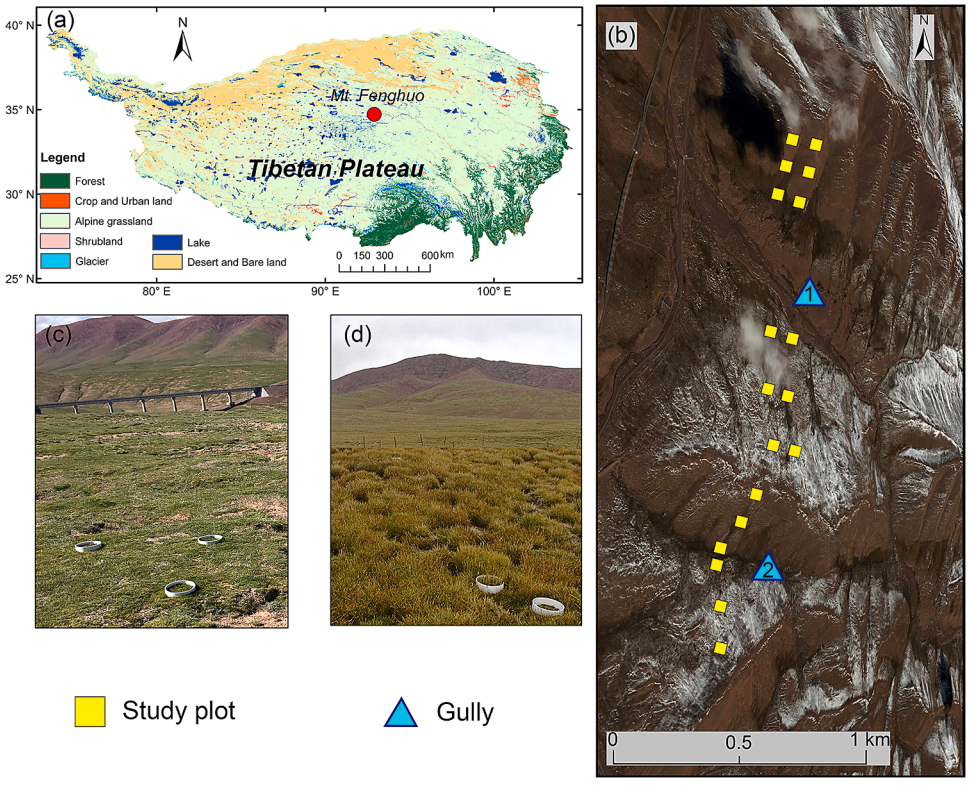

Fig. 1. Location of the study area and plots in a Tibetan alpine grassland. (a) Tibetan Plateau vegetation-type map (Xu, 2019) showing the study area location. (b) Eighteen study plots at three altitudinal positions on two slope aspects in two gullies (the 3D topographic map was downloaded from Google Earth). (c) Alpine meadow on the hillsides. (d) Alpine swamp meadow at lower slope position on the sunny slope.

Table 1
Selected characteristics and rates of ecosystem respiration (Re) and methane (CH_4) fluxes on two slope aspects at three altitudinal positions in a Tibetan alpine grassland. The Re and CH_4 fluxes are averages for two growing seasons (2017 and 2018).

Slope aspect	Altitudinal position	Elevation (m)	Re (g CO_2 m^{-2} d^{-1})	CH_4 fluxes (μg CH_4 m^{-2} h^{-1})	Dominant species
Shady slope	Lower	4745	7.32 ± 1.06	−3.37 ± 0.66	*Kobresia humilis*
	Middle	4810	6.46 ± 0.37	−10.48 ± 0.78	*K. humilis and K. pygmaea*
	Upper	4875	4.57 ± 0.49	−7.29 ± 0.92	*K. pygmaea*
Sunny slope	Lower	4745	6.02 ± 0.53	−1.60 ± 0.88	*K. tibetica and K. humilis*
	Middle	4810	6.18 ± 0.45	−7.31 ± 0.72	*K. humilis and K. pygmaea*
	Upper	4875	6.21 ± 0.62	−8.48 ± 0.62	*K. pygmaea and Oxytropis sp*

soil collars (diameter: 20.3 cm; height: 10 cm; and depth: 5 cm) were placed in each study plot to measure Re and CH_4 fluxes. Therefore, we set up three study plots under the same terrain conditions in two gullies (replicated in Gully 1) and installed a total of 54 polyvinyl chloride collars across the 18 study plots.

2.2. Measurement of ecosystem respiration and methane fluxes

An ultra-portable greenhouse gas analyser (LGR-UGGA, ABB, Canada) equipped with a measurement control system (PS-3000, LICA United Technology Limited, China) and a portable automatic dark chamber (SC-11, LICA United Technology Limited, China) was used to measure the Re and CH_4 fluxes (Supplementary methods; Fig. S3). The instrument can simultaneously determine the soil temperature and soil volumetric water content at a depth of 10 cm directly adjacent the polyvinyl chloride collar using a sensor (CS655, Campbell Scientific, USA) while measuring Re and CH_4 fluxes. We measured the Re and CH_4 fluxes during the growing seasons (June to October) of 2017 and 2018, approximately once every 30 days. Based on the methodology used in previous studies conducted at sites near our study area (Yu et al., 2013; Wei et al., 2015a; Peng et al., 2019; Li et al., 2020), the Re and CH_4 fluxes were measured between 10:00 a.m. and 11:30 a.m. (UTC +8) to represent the daily average rates of Re and CH_4 fluxes. Specifically, we measured the Re and CH_4 fluxes of the study plots at all three altitudinal positions on one slope on one day and completed the measurements for all 18 study plots within four days.

2.3. Plant and soil analyses

Two subplots (50 × 50 cm) at each study plot were demarcated for collection of aboveground biomass. This was accomplished by clipping all plants in each subplot to soil surface level in early September 2018. Below-ground (root) biomass was collected from each subplot in four separate layers (0–10, 10–20, 20–30, and 30–40 cm) using a soil corer (5 cm in diameter). The harvested above- and below-ground plant biomass was oven-dried at 60 °C for 48 h and weighed.

In mid-August 2018, samples from the top 10 cm of the soil at each of the 18 study plots were collected using a soil drill (3 cm in diameter). Three soil cores were collected from three random locations at each study plot and mixed to provide one composite soil sample per plot. All soil samples were passed through a 2 mm sieve in preparation for further analysis. Each composite soil sample was divided into two subsamples. One subsample from each plot was air-dried to enable analysis of soil organic matter and pH. The air-dried samples were sieved through 0.15 mm sieves, inorganic carbon was removed using HCl, and the concentrations of soil organic carbon and soil total nitrogen were measured using an elemental analyser (Vario Macro Cube, Elementar, Germany). The pH of the soil was determined using a pH electrode (HASH, HQ30D, America) in a 2.5:1 soil/water suspension (w/v). In addition, the soil bulk density was determined based on the method described by Chang et al. (2015). Bulk density values were used to calculate the soil water-filled pore space following the method of Yang et al. (2018).

The other subsamples were stored at 4 °C and transported to a laboratory as quickly as possible for further analysis. Dissolved organic carbon was extracted by mixing 10 g of fresh soil with 2 mol L^{-1} KCl for 1 h at a soil: solution (w/v) ratio of 1: 5 (Jones and Willett et al., 2006). The extract was then filtered through a 0.45-μm PTFE membrane and analysed using a liquid carbon and nitrogen analyser (Vario TOC Select, Elementar, Germany). Microbial biomass carbon and microbial biomass nitrogen were determined using the chloroform fumigation-extraction method (Wu et al., 1990), with a 1: 4 soil: solution for extraction with 0.5 mol L^{-1} K_2SO_4. The extraction coefficients were 0.45 and 0.54 for microbial biomass carbon and microbial biomass nitrogen, respectively (Beck et al., 1997; Riggs and Hobbies 2016). The soil saccharase activity was determined by colorimetry using 3,5-dinitrosalicylic acid as a substrate, after Guan et al. (1986). The concentrations of NH_4^+-N and NO_3^--N were determined from extracts obtained by mixing 10 g of fresh soil with 50 mL of KCl solution (1 mol L^{-1}) that were analysed using a flow injection analyser (AutoAnalyser3, Seal, Germany).

2.4. Data analysis

We analysed the data in three steps. First, we established a mixed linear model to examine the differences in Re and CH_4 fluxes under the different terrain conditions of the two gullies. The slope aspects (two levels: shady and sunny slopes), altitudinal positions (three levels: lower, middle, and upper slope positions), and their interactions were treated as fixed factors; the sampling date and polyvinyl chloride collars (replicates) were treated as random factors. The Re and CH_4 fluxes were compared with respect to slope aspect and altitudinal position using Tukey's honestly significant difference (HSD) test. The mixed linear model was established using R (version 3.5.1) with the *lme4* package (Bates et al., 2015). In addition, two-way analysis of variance with Tukey's HSD test and the Kruskal–Wallis test with Dunn's test were performed to compare the differences among the abiotic and biotic factors across the gullies.

Second, ordinary least squares regression was applied to explore the relationships of the Re and CH_4 fluxes with influencing factors; specifically, we used mean values of Re and CH_4 fluxes, soil temperature, and soil volumetric water content determined by interpolating the daily average values between sampling dates (Zhang et al., 2017), as well as the mean values of other factors recorded in August 2018. We selected the equation with the lowest Akaike information criterion score as the fitted equation.

Third, we used variation partitioning analysis with *vegan* package (Oksanen, 2011) to determine the relative importance of the factors that influence Re of the alpine grassland at the watershed scale. Negative values in variation partitioning analysis indicate that the explanatory variables account for less variation than the random normal variables (Legendre, 2008). The group that has negative value in variation partitioning analysis could be explained by the fact that the variation in Re was interpreted as zero (Legendre, 2008; Chen et al., 2019). Furthermore, we conducted structural equation modelling with *piecewiseSEM* package (Lefcheck, 2016) to evaluate the direct and indirect relationships between Re and the influencing factors. Principal component analysis was conducted to create a multivariate functional index because the soil organic matter (soil organic carbon and total nitrogen) and microbial factors (represented by microbial biomass carbon and nitrogen and soil saccharase activity) groups were closely correlated (Fig. S4). The first component (PC1), which explained 76–98% of the

total variance in soil organic matter and microbial factors, was introduced as a new variable in the subsequent structural equation modelling analysis (Table S1). When a variable followed a significant linear regression with the average Re ($p < 0.05$), it could enter the variation partitioning analysis and structural equation modelling. All data were shown as the mean ± 1 standard error.

3. Results

3.1. Abiotic and biotic factors

The soil temperature exhibited an evident seasonal variation, peaking at 11.9 °C in July, whereas the soil volumetric water content showed limited seasonal fluctuation except for a marked decrease in October (Fig. S5). The soil temperature was higher on the sunny than on the shady slope, whereas the soil volumetric water content exhibited limited differences between the two slopes (Table S2; Fig. S6a, b). Soil temperature and soil volumetric water content were significantly higher at the lower than at the middle and upper positions on both slopes (Fig. S6a, b).

The plant biomass and soil biophysiochemical factors (including soil organic carbon, soil total nitrogen, dissolved organic carbon, microbial biomass carbon, microbial biomass nitrogen, and saccharase activity) were not significantly different between the shady and sunny slopes (Table S2; Fig. S7). Although the altitudinal position significantly affected the concentration of dissolved organic carbon only on the sunny slope, other factors had relatively higher values at the lower slope positions compared to the other altitudinal positions (Fig. S7).

3.2. Seasonal variation in ecosystem respiration and methane fluxes

During both growing seasons, all study plots generally showed negative CH_4 fluxes, suggesting CH_4 sinks and net CH_4 uptake (Fig. 2d–f), with an average of -6.42 ± 0.78 μg CH_4 m^{-2} h^{-1}. Both the Re and net CH_4 uptake rates increased from June to August and decreased in September and October (Fig. 2). The seasonal variation in Re was mainly related to soil temperature (Fig. S8), whereas the seasonal variation in net CH_4 uptake rates showed a positive correlation with the soil temperature, but a negative correlation with soil volumetric water content (Fig. S9).

3.3. Variation in ecosystem respiration and methane fluxes at the watershed scale

The average Re ranged from 4.57 to 7.32 g CO_2 d^{-1} across the gullies (Table 1). There was no significant difference in Re between the shady and sunny slopes (Fig. 2g). On the sunny slope, Re was similar at different altitudinal positions, whereas on the shady slope, the Re at the lower slope positions were significantly higher than at the upper slope positions (Fig. 2g).

The average CH_4 flux rates ranged from −1.60 to −10.48 μg CH_4 m^{-2} h^{-1} across the gullies (Table 1). The middle and upper slope positions on the shady and sunny slopes showed no significant differences in CH_4 fluxes (Fig. 2h); however, the middle and upper slope positions net CH_4 uptake rates were higher than those at the lower slope positions (Fig. 2h; Table 1).

3.4. Relationships of ecosystem respiration and methane fluxes with biophysiochemical factors at the watershed scale

Ecosystem respiration increased linearly with an increase in soil temperature, soil organic carbon, soil total nitrogen, microbial biomass carbon, microbial biomass nitrogen, and saccharase activity (Fig. 3). However, Re increased and then decreased with an increase in soil volumetric water content and concentration of dissolved organic carbon (quadratic relationship, Fig. 3b, e). In addition, there was no relationship between Re and plant biomass across the gullies (Fig. 3i). Variation partitioning analysis revealed that the microbial factor was the primary contributor to the spatial variability in Re at the watershed scale (47.0%, indicated as C + AC + BC + ABC), followed by soil organic matter (31.8%, B + AB + BC + ABC) and soil temperature (18.1%, A + AB + AC + ABC). These three groups accounted for 45.0% of the variation (Fig. 4a). Noticeably, the interactive effects of the three groups accounted for a much greater proportion of Re variance than the effect of each independent factor (Fig. 4a). Furthermore, structural equation modelling showed that the microbial factor had a direct effect on Re, whereas soil organic matter and soil temperature indirectly affected Re by altering the microbial factor (Fig. 4b).

The net CH_4 uptake rates decreased with increasing soil volumetric water content ($r^2 = 0.76$, $p < 0.01$; Fig. 5b) and water-filled pore space ($r^2 = 0.60$, $p < 0.01$; Fig. 5c). Moreover, there was a close positive correlation between soil volumetric water content and water-filled pore space ($r = 0.77$, $p < 0.01$; Fig. S10a). Conversely, CH_4 fluxes showed a nonlinear quadratic relationship with soil temperature ($r^2 = 0.51$, $p < 0.01$; Fig. 5a). In our study area, the concentrations of NH_4^+-N and NO_3^--N had limited effects on the CH_4 fluxes of the alpine grassland across the gullies (Fig. 5d, e). We did not find a significant relationship between CH_4 fluxes and Re (Fig. S10b).

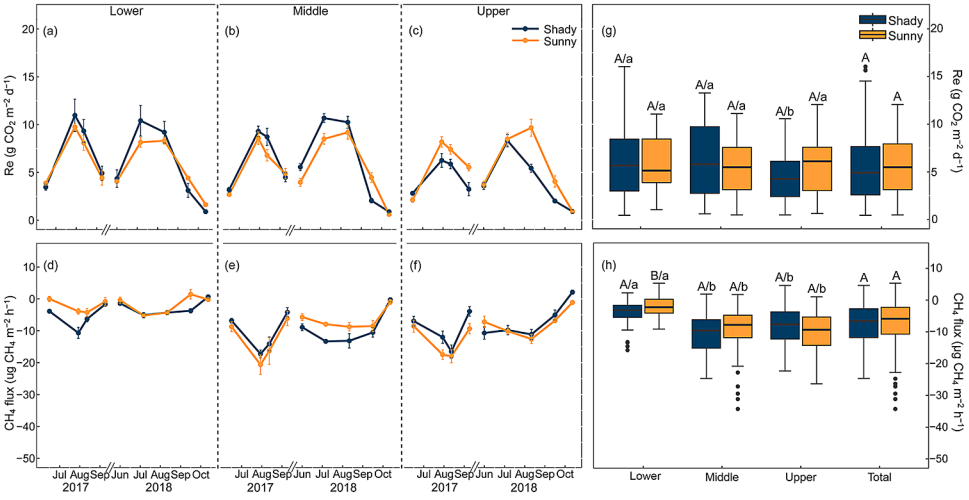

Fig. 2. Tibetan alpine grassland watershed scale seasonal variation in the rates of ecosystem respiration (Re) (a–c) and methane (CH_4) fluxes (d–f) and their ranges (g and h) during two growing seasons. In panels (a)–(f), the bars represent the standard error of each mean. In panels (g) and (h), *Total* represents data for all three altitudinal positions for same slope aspect. In the boxplots, the outer edges and horizontal lines are the 25th, 75th, and 50th quantiles, respectively. The whiskers and black circles represent a range of 1.5 times within the interquartile range and outliers, respectively. The different uppercase letters represent significant differences ($P < 0.05$) between the shady and sunny slopes at the same altitudinal position. The different lowercase letters represent significant differences among different altitudinal positions for the same slope aspect.

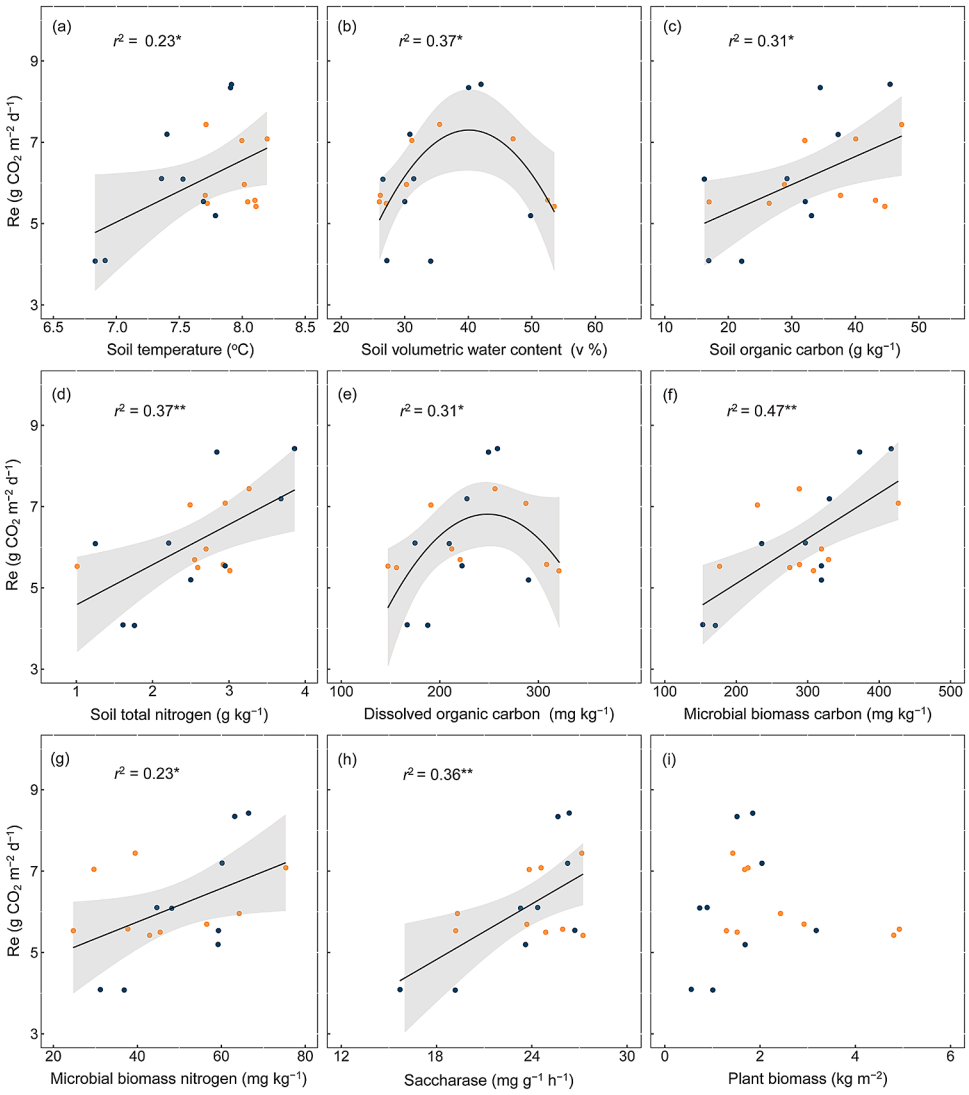

Fig. 3. Relationships between ecosystem respiration (Re) and biophysiochemical factors across watersheds in a Tibetan alpine grassland. The asterisk (*) represents $0.01 < p < 0.05$ and the double asterisks (**) represents $p < 0.01$.

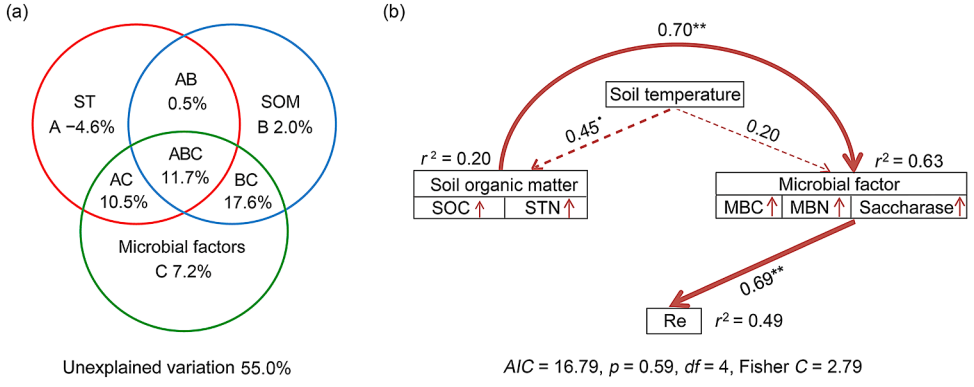

Fig. 4. Variation partitioning analysis (a) and structural equation modelling (b) examining the multivariate effects of driving factors on ecosystem respiration (Re) across watersheds in a Tibetan alpine grassland. In panel (a), ST represents soil temperature and SOM represents soil organic matter. In panel (b), the solid arrows indicate significant relationships ($p < 0.05$); the dashed arrows indicate insignificant relationships ($p > 0.05$); and arrow width is proportional to the strength of the relationship. Multiple-layer rectangles represent the first component of the principal component analysis conducted for soil organic matter and the microbial factor; soil organic matter includes soil organic carbon (SOC) and soil total nitrogen (STN), and the microbial factor includes microbial biomass carbon (MBC), microbial biomass nitrogen (MBN), and saccharase activity (Table S1). The double asterisks (**) represent $p < 0.01$ and the superscript dot (·) represents $0.1 < p < 0.05$.

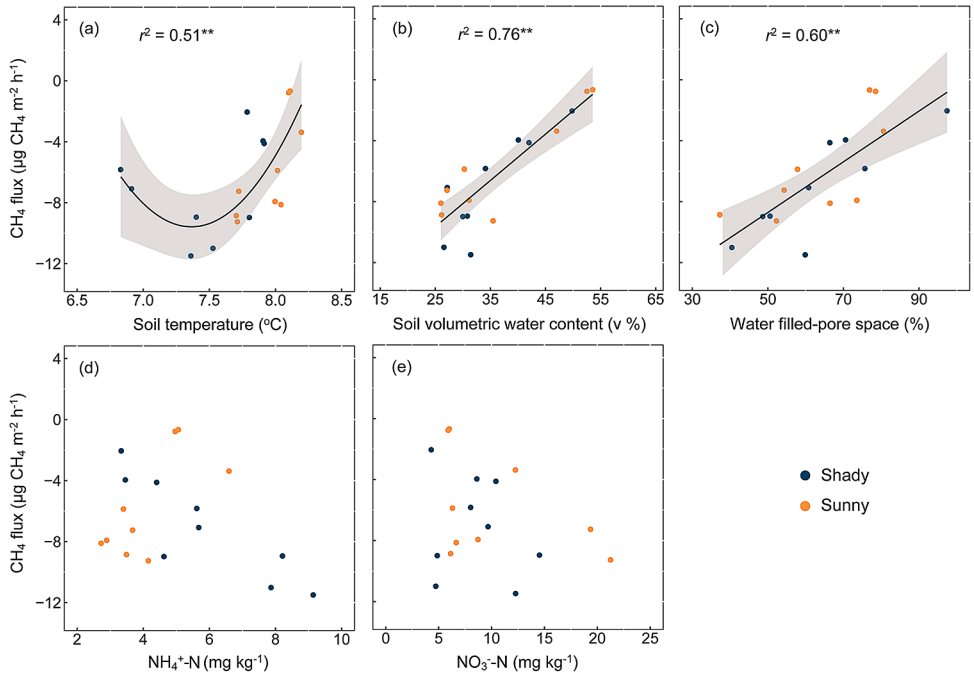

Fig. 5. Relationships between methane (CH_4) flux rates and soil temperature (a), soil volumetric water content (b), water-filled pore space (c), and the concentrations of NH_4^+-N (d) and NO_3^--N (e) across watersheds in a Tibetan alpine grassland. The double asterisks (**) represents $p < 0.01$.

4. Discussion

4.1. Growing season ecosystem respiration and methane fluxes

The average Re over the growing seasons of 6.13 ± 0.29 g CO_2 m^{-2} d^{-1} in the alpine grassland in our study area was similar to that in the Dangxiong alpine meadow (from 3.99 to 10.68 g CO_2 m^{-2} d^{-1} along an altitudinal gradient), but lower than that of 13.16 ± 1.14 g CO_2 m^{-2} d^{-1} in the Haibei alpine meadow (Jiang et al., 2010; Zhao et al., 2017). The fact that Re was greater in the Haibei alpine meadow might be attributed to a higher mean annual temperature at this location (Table S3; Zhang et al., 2017). The potential impact of soil temperature on Re is also reflected at a global scale, where the rate of Re in the Tibetan alpine permafrost region is close to that in the Arctic tundra (Tables S3 and S4), and lower than in temperate grasslands; these differences may be related to the lower soil temperatures in the Tibetan Plateau and the Arctic permafrost regions (Yuan et al., 2011). In our study, the seasonal pattern of Re was mainly determined by changes in soil temperature at all study plots (Fig. S8), which is consistent with most field observations (Luo et al., 2001; Li et al., 2015).

In alpine grassland located near our study area, Chen et al. (2017) have recorded CH_4 uptake rates with seasonal averages of −12.12 ± 0.42 μg CH_4 m^{-2} h^{-1} in alpine meadow and −3.41 ± 1.08 μg CH_4 m^{-2} h^{-1} in alpine swamp meadow, which are consistent with our findings. However, compared to CH_4 fluxes in other alpine meadows on the Tibetan Plateau, the higher soil volumetric water content and lower soil temperature in our study area may have caused the gully soils we studied to be weak sinks of atmospheric CH_4 (Table S3; Wei et al., 2015a). Research in the Arctic upland tundra supports this explanation, as it is reported that dry tundra with a lower soil volumetric water content and higher soil temperature has higher net CH_4 uptake rates than moist tundra (Jørgensen et al., 2015). Warming and drying have been found to significantly increase the abundance of methanotrophic communities and CH_4 oxidation (Zheng et al., 2012; Natali et al., 2015, 2018), which further explains the greater net CH_4 uptake rates associated with lower soil volumetric water content and higher soil temperature that we observed in August in our study (Fig. 2d–f; Fig. S5). In the context of climate change, a synergistic increase in temperature and precipitation on the Tibetan Plateau would add uncertainty to the prediction of CH_4 fluxes in Tibetan alpine grassland (Wang et al., 2008a; Piao et al., 2019).

4.2. Control of ecosystem respiration at the watershed scale

Ecosystem respiration encompasses autotrophic respiration from plants and heterotrophic respiration from soil microbes (Natali et al., 2014; Zhang et al., 2017). In our study area, autotrophic respiration and heterotrophic respiration account for 35% and 65% of the soil respiration, respectively (Zhang, 2016). Meanwhile, considering that the root biomass of alpine grasslands account for 86–96% of total plant biomass (Li et al., 2011), we believe that Re mainly comes from heterotrophic respiration in our study area. The much lower percentage of autotrophic respiration may be the reason why we did not find a significant relationship between plant biomass and Re across the watersheds (Fig. 3i). On the other hand, the microbial factor, consisting of microbial biomass carbon and nitrogen and saccharase activity, were identified as the direct and primary control over the spatial variability in Re at the watershed scale (Fig. 4). The strong interactions between the microbial factor and soil temperature or soil organic matter (Fig. 4a), suggested that the effect of the microbial factors on Re depends on the soil temperature and soil organic matter content (Treat et al., 2014; Shi et al., 2017). It has been well documented that a high soil temperature and high soil organic matter content are favourable for greater microbial activity and thus the generation of larger Re (Xue et al., 2016; Chen et al., 2019). In relative to other positions, soil temperature is lower at the upper positions on the shady slopes; the soil organic matter content was also lower likely due to soil erosion caused by running water. As a result, the observed microbial activity and Re were lower at the upper positions on the shady slopes (Fig. 2g; Sommerkorn, 2008).

Although not included as a variable for variation partitioning analysis and structural equation modelling due to the non-linear relationship between soil volumetric water content and Re (Fig. 3b), the Re was also influenced by soil volumetric water content at the watershed scale of this Tibetan alpine grassland. An excessive soil volumetric water content (> 40%) in the lower slope could reduce the diffusivity of oxygen in these soils, resulting in a reduced microbial decomposition and thus a

moderate Re (Xu and Qi, 2001; Hu et al., 2008), even at higher soil temperatures and soil organic matter content (Fig. S6 and S7). Low soil permeability in this permafrost region reduces the infiltration of moisture into the soil, which generally leads to the formation of poorly drained landscapes at the lower slope positions (Metcalfe and Buttle, 2001). On the sunny slope, the deeper upslope thawing depth may lead to more soil water flowing down the slope (Fig. S2), resulting in even higher soil volumetric water content in the lower slope position (Fig. S6b). The spatial variability in soil volumetric water content caused by terrain has also been identified as an important factor influencing Re in Arctic tundra (Grant et al., 2017). Differences in topography and active layer depth are known to change the upslope hydrological conditions and form water tracks in upland tundra, which cause spatial variability in Re at the landscape scale (Chapin et al., 1988; Curasi et al., 2016). Lower Re values have been recorded from the lower centres than from the higher rims in polygons in the Arctic landscape, mainly because the excessive soil volumetric water content suppressed Re in the lower landform centres (Zona et al., 2011; Vaughn et al., 2016). Our findings suggest that microbial activity is the primary control on Re, while terrain position determined soil volumetric water content, soil organic matter content and soil temperature interact with microbial factors to drive the watershed scale variability in Re in the alpine grassland we studied.

4.3. Control of methane fluxes at the watershed scale

The soil volumetric water content had a definite effect on the alpine grassland CH_4 fluxes at the watershed scale (Fig. 5b). A similar effect of soil volumetric water content on CH_4 fluxes has been observed at other spatial scales in Tibetan alpine grassland and in the Arctic tundra. For example, at a microtopography scale, Christensen et al. (2000) and Wei et al. (2015b) recorded distinct spatial heterogeneity of CH_4 fluxes associated with hollow terrain and hummocks because of differences in the soil volumetric water content (Tables S3 and S4). On a regional scale, the net CH_4 uptake rates display a decreasing trend from dry to wet sites with an increase in the soil volumetric water content (Emmerton et al., 2014; Jørgensen et al., 2015; McEwing et al., 2015; Zhang et al., 2019). As mentioned in the Section 4.1, the methanotrophic community prefers aerobic conditions; thus, net CH_4 uptake rates decrease with an increase in the soil volumetric water content (Jørgensen et al., 2015; Wei et al., 2015a). Therefore, a higher soil volumetric water content at the lower slope positions may have reduced the abundance of the methanotrophic community and resulted in lower net CH_4 uptake rates than those at the other altitudinal positions (Fig. 2h). Affected by global warming, the thickness of the active layer in the permafrost regions of the Tibetan Plateau continues to deepen (Cheng et al., 2019), which may lead to further reduction in soil volumetric water content in the topsoil of the upper mountain slopes (McGuire et al., 2002; Li, 2010; Cheng et al., 2019), and may further increase the difference in CH_4 fluxes between the upper and lower slope positions. In the mid-region of the sunny slope, a higher soil bulk density may have caused an increase in the soil water-filled pore space, thereby reducing the oxidation of CH_4 (Fig. S6c, d; Dunfield et al., 2007; Yang et al., 2018). This could account for why the net CH_4 uptake rates at the middle altitudinal positions on the sunny slope were lower than at the same altitudinal position on the shady slope (Fig. 2h), although the difference was not significant ($p > 0.05$).

The CH_4 fluxes we obtained showed a nonlinear quadratic relationship with soil temperature at the watershed scale, which is inconsistent with the phenomenon that net CH_4 uptake rates increase with an increase in soil temperature at the locale scale (Jørgensen et al., 2015; Natali et al., 2015). This may be because higher soil moisture, which is synchronous with higher soil temperature in the topsoil of the lower slope positions, has a greater effect on the suppression of CH_4 oxidation and restrained the effect of the soil temperature in our study area. Similarly, by performing a warming experiment on different alpine grassland types, Li et al. (2020) demonstrated that the effect of soil temperature on CH_4 fluxes is related to the soil volumetric water content. Previous studies on the Tibetan Plateau have found that net CH_4 uptake rates are influenced by the concentrations of NH_4^+-N and NO_3^--N (Peng et al., 2019). Specifically, the appropriate addition of nitrogen could increase the activity of methanotrophs, given that the Tibetan alpine permafrost region is a naturally N-limited region (Kou et al., 2017, 2020). However, we did not observe a significant relationship between NH_4^+-N or NO_3^--N and net CH_4 uptake rates in our study, although the concentrations of NH_4^+-N and NO_3^--N ranged widely across the gullies (Fig. 5d and e). Overall, we highlighted the significant effect of soil moisture in controlling alpine grassland CH_4 fluxes at the watershed scale.

Our study inevitably improves the understanding of watershed scale patterns and controlling factors of Re and CH_4 fluxes in the Tibetan alpine permafrost region. However, some limitations still exist and need to be addressed in future studies. First, the monthly measurements of Re and CH_4 fluxes do not capture the diurnal variations of Re and CH_4 fluxes of the study area. A highly time-resolved (e.g. diurnal) fluxes dataset can accurately describe temporary changes within watersheds and can be obtained using the continuous automated trace gas analyser with multiplexer. Second, as our experiments were conducted in growing seasons only, the patterns of Re and CH_4 fluxes of the non-growing season were missing. Non-growing season Re was found to account for about 25% of annual Re (Zhang et al., 2015; Zhu et al., 2020) and non-growing season CH_4 uptake contribute to about 13% of annual CH_4 fluxes in an alpine grassland (Li et al., 2012; Li, 2013), suggesting that non-growing season fluxes should not be overlooked in future flux measurements. Finally, although dark chambers are frequently used to measure CH_4 fluxes (Wei et al., 2015b; Peng et al., 2019), there are also studies showing that the absence of light under a dark chamber may influence CH_4 fluxes by altering soil oxygen availability and the allocation of recent photosynthate to belowground microorganisms (von Fischer et al., 2010; Li et al., 2016; Bao et al., 2020).

5. Conclusion

Our two-year Tibetan alpine grassland field study revealed that altitudinal position significantly affected CH_4 fluxes owing to differences in soil moisture along the gully slopes within the watersheds. Abiotic and microbial factors interactively affected Re, and the microbial factor had a direct and regulated effect on Re at the watershed scale. Our results show that the influence of permafrost on hill slope hydrology may further increase spatial heterogeneity of soil moisture, which can potentially alter the carbon exchange of alpine grassland at the watershed scale, especially considering the weaker CH_4 net uptake rates at the lower slope positions than at the other slope positions. These findings have important implications for estimating carbon exchange in the mountains of the Tibetan permafrost regions. Given that mountains cover approximately 60.58% of the Tibetan Plateau, neglecting spatial variability in Re and CH_4 fluxes at the watershed scale may mislead the assessment of carbon exchange. Hence, we recommend that spatial variability in Re and CH_4 fluxes at the watershed scale should be considered in the earth system model to improve the evaluation of carbon exchange in Tibetan alpine grassland.

Declaration of Competing Interest

The authors declare that they have no known competing financial interests or personal relationships that could have appeared to influence the work reported in this paper.

Acknowledgments

This work was supported by the National Key Research and Development Program of China (2016YFC0502105); National Natural Science

Foundation of China (41671206); the Youth Innovation Promotion Association CAS, China (2018406).

Supplementary materials

Supplementary material associated with this article can be found, in the online version, at doi:10.1016/j.agrformet.2021.108451.

References

Bao, T., Zhu, R., Ye, W., et al., 2020. Effects of sunlight on tundra nitrous oxide and methane fluxes in maritime Antarctica. Adv. Polar Sci. 31 (3), 178–191. https://doi.org/10.13679/j.advps.2020.0005.

Bates, D., Maechler, M., Bolker, B.M., et al., 2015. Fitting linear mixed-effects models using lme4. J. Stat. Softw. 67 (1), 1–48. https://doi.org/10.18637/jss.v067.i01.

Beck, T., Joergensen, R.G., Kandeler, E., et al., 1997. An inter-laboratory comparison of ten different ways of measuring soil microbial biomass C. Soil Biol. Biochem. 29 (7), 1023–1032. https://doi.org/10.1016/S0038-0717(97)00030-8.

Bockheim, J.G., Munroe, J.S, 2014. Organic carbon pools and genesis of alpine soils with permafrost: a review. Arct. Antarct. Alp. Res. 46 (4), 987–1006. https://doi.org/10.1657/1938-4246-46.4.987.

Cao, W., Tao, H., Kong, B., et al., 2011. Recognition of general topographic features in Qinghai-Tibet Plateau based on GIS. Bull. Soil Water Conserv. 31 (4), 163–167. https://doi.org/10.13961/j.cnki.stbctb.2011.04.004.

Carletti, P., Vendramin, E., Pizzeghello, D., et al., 2009. Soil humic compounds and microbial communities in six spruce forests as function of parent material, slope aspect and stand age. Plant Soil 315 (1–2), 47–65. https://doi.org/10.1007/s11104-008-9732-z.

Chang, R., Wang, G., Fei, R., et al., 2015. Altitudinal change in distribution of soil carbon and nitrogen in Tibetan montane forests. Soil Sci. Soc. Am. J. 79 (5), 1455–1469. https://doi.org/10.2136/sssaj2015.02.0055.

Chapin, F.S., Fetcher, N., Kielland, K., et al., 1988. Productivity and nutrient cycling of Alaskan tundra: enhancement by flowing soil-water. Ecology 69 (3), 693–702. https://doi.org/10.2307/1941017.

Chen, L., Liu, L., Qin, S., et al., 2019. Regulation of priming effect by soil organic matter stability over a broad geographic scale. Nat. Commun. 10 (1), 5112. https://doi.org/10.1038/s41467-019-13119-z.

Chen, X., Wang, G., Zhang, T., et al., 2017. Effects of warming and nitrogen fertilization on GHG flux in an alpine swamp meadow of a permafrost region. Sci. Total Environ. 601, 1389–1399. https://doi.org/10.1016/j.scitotenv.2017.06.028.

Cheng, G., Zhao, L., Li, R., et al., 2019. Characteristic, changes and impacts of permafrost on Qinghai-Tibet Plateau. Chin. Sci. Bull. 64 (27), 2783–2795. https://doi.org/10.1360/TB-2019-0191. Chinese.

Christensen, T.R., Friborg, T., Sommerkorn, M., et al., 2000. Trace gas exchange in a high-arctic valley 1. Variations in CO_2 and CH_4 flux between tundra vegetation types. Glob. Biogeochem. Cycles 14 (3), 701–713. https://doi.org/10.1029/1999GB001134.

Curasi, S.R., Loranty, M.M., Natali, S.M, 2016. Water track distribution and effects on carbon dioxide flux in an eastern Siberian upland tundra landscape. Environ. Res. Lett. 11 (0450024) https://doi.org/10.1088/1748-9326/11/4/045002.

Ding, J., Wang, T., Piao, S., et al., 2019. The paleoclimatic footprint in the soil carbon stock of the Tibetan permafrost region. Nat. Commun. 10 (1), 4195. https://doi.org/10.1038/s41467-019-12214-5.

Dunfield, P.F., Yuryev, A., Senin, P., et al., 2007. Methane oxidation by an extremely acidophilic bacterium of the phylum Verrucomicrobia. Nature 450 (7171), 879–882. https://doi.org/10.1038/nature06411.

Emmerton, C.A., St Louis, V.L., Lehnherr, I., et al., 2014. The net exchange of methane with high Arctic landscapes during the summer growing season. Biogeosciences 11 (12), 3095–3106. https://doi.org/10.5194/bg-11-3095-2014.

Fan, Y., Clark, M., Lawrence, D.M., et al., 2019. Hillslope hydrology in global change research and earth system modeling. Water Resour. Res. 55 (2), 1737–1772. https://doi.org/10.1029/2018WR023903.

Grant, R.F., Mekonnen, Z.A., Riley, W.J., et al., 2017. Mathematical modelling of Arctic polygonal tundra with ecosys: 2. Microtopography determines how CO_2 and CH_4 exchange responds to changes in temperature and precipitation. J. Geophys. Res.: Biogeosci. 122 (12), 3174–3187. https://doi.org/10.1002/2017JG004037.

Guan, S., Zhang, D., Zhang, Z., 1986. Soil Enzymes and Their Research Methods. Agriculture Press, Beijing, pp. 291–294.

Hu, Q., Wu, Q., Cao, G.M., et al., 2008. Growing season ecosystem respirations and associated component fluxes in two alpine meadows on the Tibetan Plateau. J. Integr. Plant Biol. 50 (3), 271–279. https://doi.org/10.1111/j.1744-7909.2007.00617.x.

IPCC, 2013. Climate Change 2013: The Physical Science Basis; Contribution of Working Group I to the Fifth Assessment Report of the Intergovernmental Panel on Climate Change. Cambridge University Press, Cambridge/New York.

Jiang, C., Yu, G., Fang, H., et al., 2010. Short-term effect of increasing nitrogen deposition on CO_2, CH_4 and N_2O fluxes in an alpine meadow on the Qinghai-Tibetan Plateau, China. Atmos. Environ. 44 (24), 2920–2926. https://doi.org/10.1016/j.atmosenv.2010.03.030.

Jørgensen, C.J., Lund Johansen, K.M., Westergaard-Nielsen, A., et al., 2015. Net regional methane sink in high arctic soils of northeast Greenland. Nat. Geosci. 8 (1), 20–23. https://doi.org/10.1038/ngeo2305.

Jones, D.L., Willett, V.B, 2006. Experimental evaluation of methods to quantify dissolved organic nitrogen (DON) and dissolved organic carbon (DOC) in soil. Soil Biol. Biochem. 38 (5), 991–999. https://doi.org/10.1016/j.soilbio.2005.08.012.

Kou, Y., Li, J., Wang, Y., et al., 2017. Scale-dependent key drivers controlling methane oxidation potential in Chinese grassland soils. Soil Biol. Biochem. 111, 104–114. https://doi.org/10.1016/j.soilbio.2017.04.005.

Kou, D., Yang, G., Li, F., et al., 2020. Progressive nitrogen limitation across the Tibetan alpine permafrost region. Nat. Commun. 11 (33311) https://doi.org/10.1038/s41467-020-17169-6.

Lefcheck, J.S, 2016. PiecewiseSEM: piecewise structural equation modelling in R for ecology, evolution, and systematics. Methods Ecol. Evol. 7 (5), 573–579. https://doi.org/10.1111/2041-210X.12512.

Legendre, P., 2008. Studying beta diversity: ecological variation partitioning by multiple regression and canonical analysis. J. Plant Ecol. 1 (1), 3–8. https://doi.org/10.1093/jpe/rtm001.

Lessovaia, S.N., Goryachkin, S.V., Desyatkin, R.V., et al., 2013. Pedoweathering and mineralogical change in cryosols in an ultra-continental climate (Central Yakutia, Russia). Acta Geodyn. Geomater. 10 (4), 465–473. https://doi.org/10.13168/AGG.2013.0047.

Li, C., 2010. The Experimental Study of the Impact of Alpine grassland Coverage Changes on the Surface Hydrological Cycle at Permafrost Zone of the Qinghai-Tibet Plateau. Lanzhou University, p. 42.

Li, F., Yang, G., Peng, Y., et al., 2020. Warming effects on methane fluxes differ between two alpine grasslands with contrasting soil water status. Agric. For. Meteorol. 290, 107988 https://doi.org/10.1016/j.agrformet.2020.107988.

Li, F., Zhu, R., Bao, T., et al., 2016. Sunlight stimulates methane uptake and nitrous oxide emission from the High Arctic tundra. Sci. Total Environ. 572, 1150–1160. https://doi.org/10.1016/j.scitotenv.2016.08.026.

Li, K., 2013. Responses of Plant Community and Greenhouse Gas Emission to Elevated N deposition in Alpine Grassland in Xinjiang, China. Xinjiang Institute of Ecology and Geography CAS, p. 65.

Li, K., Gong, Y., Song, W., et al., 2012. Responses of CH_4, CO_2 and N_2O fluxes to increasing nitrogen deposition in alpine grassland of the Tianshan Mountains. Chemosphere 88 (1), 140–143. https://doi.org/10.1016/j.chemosphere.2012.02.077.

Li, N., Wang, G.X., Yang, Y., et al., 2011. Plant production, and carbon and nitrogen source pools, are strongly intensified by experimental warming in alpine ecosystems in the Qinghai-Tibet Plateau. Soil Biol. Biochem. 43 (5), 942–953. https://doi.org/10.1016/j.soilbio.2011.01.009.

Li, Y., Dong, S., Liu, S., et al., 2015. Seasonal changes of CO_2, CH_4 and N_2O fluxes in different types of alpine grassland in the Qinghai-Tibetan Plateau of China. Soil Biol. Biochem. 80, 306–314. https://doi.org/10.1016/j.soilbio.2014.10.026.

Luo, Y., Wan, S., Hui, D., et al., 2001. Acclimatization of soil respiration to warming in a tall grass prairie. Nature 413 (6856), 622–625. https://doi.org/10.1038/35098065.

McEwing, K.R., Fisher, J.P., Zona, D, 2015. Environmental and vegetation controls on the spatial variability of CH_4 emission from wet-sedge and tussock tundra ecosystems in the Arctic. Plant Soil 388 (1–2), 37–52. https://doi.org/10.1007/s11104-014-2377-1.

McGuire, A.D., Wirth, C., Apps, M., et al., 2002. Environmental variation, vegetation distribution, carbon dynamics and water/energy exchange at high latitudes. J. Veg. Sci. 13 (3), 301–314. https://doi.org/10.1111/j.1654-1103.2002.tb02055.x.

Metcalfe, R.A., Buttle, J.M, 2001. Soil partitioning and surface store controls on spring runoff from a boreal forest peatland basin in north-central Manitoba, Canada. Hydrol. Process. 15 (12), 2305–2324. https://doi.org/10.1002/hyp.262.

Mu, C., Abbott, B.W., Norris, A.J., et al., 2020. The status and stability of permafrost carbon on the Tibetan Plateau. Earth-Sci. Rev. 211 (103433) https://doi.org/10.1016/j.earcirev.2020.103433.

Natali, S.M., Schuur, E.A.G., Webb, E.E., et al., 2014. Permafrost degradation stimulates carbon loss from experimentally warmed tundra. Ecology 95 (3), 602–608. https://doi.org/10.1890/13-0602.1.

Natali, S.M., Schuur, E.A.G., Mauritz, M., et al., 2015. Permafrost thaw and soil moisture driving CO_2 and CH_4 release from upland tundra. J. Geophys. Res.: Biogeosci. 120 (3), 525–537. https://doi.org/10.1002/2014JG002872.

Niu, Y.J., Zou, J.W., Yang, S.W., et al., 2017. Quantitative apportionment of slope aspect and altitude to soil moisture and temperature and plant distribution on alpine meadow. Chin. J. Appl. Ecol. 28 (5), 1489–1497. https://doi.org/10.13287/j.1001-9332.201705.032.

Oh, Y., Zhuang, Q., Liu, L., et al., 2020. Reduced net methane emissions due to microbial methane oxidation in a warmer Arctic. Nat. Clim. Chang. 10 (4), 317–321. https://doi.org/10.1038/s41558-020-0734-z.

Oksanen J. Multivariate Analysis of Ecological Communities in R: Vegan Tutorial. R Package Version, 2011, 1(7): 1–43.

Peng, Y., Wang, G., Li, F., et al., 2019. Unimodal response of soil methane consumption to increasing nitrogen additions. Environ. Sci. Technol. 53 (8), 4150–4160. https://doi.org/10.1021/acs.est.8b04561.

Philben, M., Tan, N., Chen, H., et al., 2020. Influences of hillslope biogeochemistry on anaerobic soil organic matter decomposition in a tundra watershed. J. Geophys. Res.: Biogeosci. 125 (7) https://doi.org/10.1029/2019JG005512.

Piao, S., Zhang, X., Wang, T., et al., 2019. Responses and feedback of the Tibetan Plateau's alpine ecosystem to climate change. Chin. Sci. Bull. 64 (27), 2842–2855. https://doi.org/10.1360/TB-2019-0074. Chinese.

Rahbek, C., Borregaard, M.K., Colwell, R.K., et al., 2019. Humboldt's enigma: what causes global patterns of mountain biodiversity? Science 365 (6458SI), 1108–1113. https://doi.org/10.1126/science.aax0149.

Riggs, C.E., Hobbie, S.E, 2016. Mechanisms driving the soil organic matter decomposition response to nitrogen enrichment in grassland soils. Soil Biol. Biochem. 99, 54–65. https://doi.org/10.1016/j.soilbio.2016.04.023.

Schuur, E.A.G., McGuire, A.D., Schädel, C., et al., 2015. Climate change and the permafrost carbon feedback. Nature 520 (7546), 171–179. https://doi.org/10.1038/nature14338.

Shi, W., Du, S., Morina, J.C., et al., 2017. Physical and biogeochemical controls on soil respiration along a topographical gradient in a semiarid forest. Agric. For. Meteorol. 247, 1–11. https://doi.org/10.1016/j.agrformet.2017.07.006.

Sommerkorn, M., 2008. Micro-topographic patterns unravel controls of soil water and temperature on soil respiration in three Siberian tundra systems. Soil Biol. Biochem. 40 (7), 1792–1802. https://doi.org/10.1016/j.soilbio.2008.03.002.

Treat, C.C., Wollheim, W.M., Varner, R.K., et al., 2014. Temperature and peat type control CO_2 and CH_4 production in Alaskan permafrost peats. Glob. Chang. Biol. 20 (8), 2674–2686. https://doi.org/10.1111/gcb.12572.

Treat, C.C., Marushchak, M.E., Voigt, C., et al., 2018. Tundra landscape heterogeneity, not interannual variability, controls the decadal regional carbon balance in the Western Russian Arctic. Glob. Chang. Biol. 24 (11), 5188–5204. https://doi.org/10.1111/gcb.14421.

Turetsky, M.R., Abbott, B.W., Jones, M.C., et al., 2020. Carbon release through abrupt permafrost thaw. Nat. Geosci. 13 (2), 138–143. https://doi.org/10.1038/s41561-019-0526-0.

Vaughn, L.J.S., Conrad, M.E., Bill, M., et al., 2016. Isotopic insights into methane production, oxidation, and emissions in Arctic polygon tundra. Glob. Chang. Biol. 22 (10), 3487–3502. https://doi.org/10.1111/gcb.13281.

von Fischer, J.C., Rhew, R.C., Ames, G.M., et al., 2010. Vegetation height and other controls of spatial variability in methane emissions from the Arctic coastal tundra at Barrow, Alaska. J. Geophys. Res.-Biogeosci. 115, G00I03. https://doi.org/10.1029/2009JG001283.

Wang, B., Bao, Q., Hoskins, B., et al., 2008a. Tibetan Plateau warming and precipitation changes in East Asia. Geophys. Res. Lett. 35 (14) https://doi.org/10.1029/2008GL034330.

Wang, G., Li, Y., Hu, H., et al., 2008b. Synergistic effect of vegetation and air temperature changes on soil water content in alpine frost meadow soil in the permafrost region of Qinghai-Tibet. Hydrol. Process 22 (17), 3310–3320. https://doi.org/10.1002/hyp.6913.

Wei, D., Ri, X., Tarchen, T., et al., 2015a. Considerable methane uptake by alpine grasslands despite the cold climate: in situ measurements on the central Tibetan Plateau, 2008–2013. Glob. Chang. Biol. 21 (2), 777–788. https://doi.org/10.1111/gcb.12690.

Wei, D., Ri, X., Tarchen, T., et al., 2015b. Revisiting the role of CH_4 emissions from alpine wetlands on the Tibetan Plateau: evidence from two in situ measurements at 4758 and 4320 m above sea level. J. Geophys. Res.: Biogeosci. 120 (9), 1741–1750. https://doi.org/10.1002/2015JG002974.

Wu, J., Joergensen, R.G., Pommerening, B., et al., 1990. Measurement of soil microbial biomass C by fumigation-extraction-an automated procedure. Soil Biol. Biochem. 22 (8), 1167–1169. https://doi.org/10.1016/0038-0717(90)90046-3.

Xu, E., 2019. Land Use of the Tibet Plateau in 2015 (Version 1.0). National Tibetan Plateau Data Center. https://doi.org/10.11888/Geogra.tpdc.270198. CSTR: 18046.11.Geogra.tpdc.270198.

Xu, M., Qi, Y., 2001. Soil-surface CO_2 efflux and its spatial and temporal variations in a young ponderosa pine plantation in northern California. Glob. Change Biol., 7 (6), 667–677. https://doi.org/10.1046/j.1354-1013.2001.00435.x.

Xue, K., Yuan, M.M., Shi, Z.J., et al., 2016. Tundra soil carbon is vulnerable to rapid microbial decomposition under climate warming. Nat. Clim. Chang. 6 (6), 595–600. https://doi.org/10.1038/nclimate2940.

Yang, G., Peng, Y., Olefeldt, D., et al., 2018. Changes in methane flux along a permafrost thaw sequence on the Tibetan Plateau. Environ. Sci. Technol. 52 (3), 1244–1252. https://doi.org/10.1021/acs.est.7b04979.

Yang, M., Nelson, F.E., Shiklomanov, N.I., et al., 2010. Permafrost degradation and its environmental effects on the Tibetan Plateau: a review of recent research. Earth-Sci. Rev. 103 (1–2), 31–44. https://doi.org/10.1016/j.earscirev.2010.07.002.

Yang, M., Wang, X., Pang, G., et al., 2019. The Tibetan Plateau cryosphere: observations and model simulations for current status and recent changes. Earth-Sci. Rev. 190, 353–369. https://doi.org/10.1016/j.earscirev.2018.12.018.

Yu, L., Wang, H., Wang, G., et al., 2013. A comparison of methane emission measurements using eddy covariance and manual and automated chamber-based techniques in Tibetan Plateau alpine wetland. Environ. Pollut. 181, 81–90. https://doi.org/10.1016/j.envpol.2013.06.018.

Yuan, W., Luo, Y.Q., Li, X., et al., 2011. Redefinition and global estimation of basal ecosystem respiration rate. Glob. Biogeochem. Cycles 25 (GB4002). https://doi.org/10.1029/2011GB004150.

Zhang, Q., Yang, G., Song, Y., et al., 2019. Magnitude and drivers of potential methane oxidation and production across the Tibetan alpine permafrost region. Environ. Sci. Technol. 53 (24), 14243–14252. https://doi.org/10.1021/acs.est.9b03490.

Zhang, T., 2016. The Effect of Experimental Warming on the Carbon Cycle of Alpine Meadow Ecosystems in the Permafrost Region of Qinghai-Tibet Plateau. Institute of Mountain Hazards and Environment, CAS, p. 86.

Zhang, T., Wang, G., Yang, Y., et al., 2015. Non-growing season soil CO_2 flux and its contribution to annual soil CO_2 emissions in two typical grasslands in the permafrost region of the Qinghai-Tibet Plateau. Eur. J. Soil Biol. 71, 45–52. https://doi.org/10.1016/j.ejsobi.2015.10.004.

Zhang, T., Wang, G., Yang, Y., et al., 2017. Grassland types and season-dependent response of ecosystem respiration to experimental warming in a permafrost region in the Tibetan Plateau. Agric. For. Meteorol. 247, 271–279. https://doi.org/10.1016/j.agrformet.2017.08.010.

Zhao, J., Li, R., Li, X., et al., 2017. Environmental controls on soil respiration in alpine meadow along a large altitudinal gradient on the central Tibetan Plateau. Catena 159, 84–92. https://doi.org/10.1016/j.catena.2017.08.007.

Zheng, Y., Yang, W., Sun, X., et al., 2012. Methanotrophic community structure and activity under warming and grazing of alpine meadow on the Tibetan Plateau. Appl. Microbiol. Biotechnol. 93 (5), 2193–2203. https://doi.org/10.1007/s00253-011-3535-5.

Zheng, J., RoyChowdhury, T., Yang, Z., et al., 2018. Impacts of temperature and soil characteristics on methane production and oxidation in Arctic tundra. Biogeosciences 15 (21), 6621–6635. https://doi.org/10.5194/bg-15-6621-2018.

Zhu, J., Zhang, F., Li, H., et al., 2020. Seasonal and interannual variations of CO_2 fluxes over 10 years in an alpine wetland on the Qinghai-Tibetan Plateau. J. Geophys. Res. Biogeosci. 125 (11) https://doi.org/10.1029/2020JG006011.

Zona, D., Lipson, D.A., Zulueta, R.C., et al., 2011. Microtopographic controls on ecosystem functioning in the Arctic Coastal Plain. J. Geophys. Res. 116 (G00I08) https://doi.org/10.1029/2009JG001241.

Zou, D., Zhao, L., Sheng, Y., et al., 2017. A new map of permafrost distribution on the Tibetan Plateau. Cryosphere 11 (6), 2527–2542. https://doi.org/10.5194/tc-11-2527-2017.